Boosting Central Nervous System Axon Regeneration by Circumventing Limitations of Natural Cytokine Signaling

Marco Leibinger[1], Anastasia Andreadaki[1], Philipp Gobrecht[1], Evgeny Levin[1], Heike Diekmann[1] and Dietmar Fischer[1]

[1]*Division of Experimental Neurology, Medical Faculty, Heinrich-Heine-University, Düsseldorf, Germany*

Retinal ganglion cells (RGCs) do not normally regenerate injured axons, but die upon axotomy. Although IL-6-like cytokines are reportedly neuroprotective and promote optic nerve regeneration, their overall regenerative effects remain rather moderate. Here, we hypothesized that direct activation of the gp130 receptor by the designer cytokine hyper-IL-6 (hIL-6) might induce stronger RGC regeneration than natural cytokines. Indeed, hIL-6 stimulated neurite growth of adult cultured RGCs with significantly higher efficacy than CNTF or IL-6. This neurite growth promoting effect could be attributed to stronger activation of the JAK/STAT3 and PI3K/AKT/mTOR signaling pathways and was also observed in peripheral dorsal root ganglion neurons. Moreover, hIL-6 abrogated axon growth inhibition by central nervous system (CNS) myelin. Remarkably, continuous hIL-6 expression upon RGC-specific AAV transduction after optic nerve crush exerted stronger axon regeneration than other known regeneration promoting treatments such as lens injury and PTEN knockout, with some axons growing through the optic chiasm 6 weeks after optic nerve injury. Combination of hIL-6 with RGC-specific PTEN knockout further enhanced optic nerve regeneration. Therefore, direct activation of gp130 signaling might be a novel, clinically applicable approach for robust CNS repair.

Received 2 March 2016; accepted 28 April 2016; advance online publication 28 June 2016. doi: 10.1038/mt.2016.102

INTRODUCTION

The adult mammalian central nervous system (CNS) shows little capacity to regenerate injured axons. This regenerative failure has been attributed to an inhibitory environment for axonal growth cones as well as an insufficient intrinsic capacity for axonal regrowth.[1–3] As a clinical consequence, functional loss after injuries to the brain or spinal cord is often irreversible and only insufficiently treatable to date. For this reason, new clinically applicable treatment strategies promoting axon regeneration are highly desirable.

Retinal ganglion cells (RGCs) are typical CNS neurons and as such do not normally regenerate injured axons after optic nerve injury. Upon axotomy, more than 80% of murine RGCs undergo apoptotic cell death within 21 days.[4–6] However, significant neuroprotection and axonal regeneration is achieved by inflammatory stimulation (IS), which can be induced in rodents, for example, by lens injury or intravitreal application of Pam_3Cys or zymosan.[7–13] Besides several cell types of the innate immune response, IS also activates astrocytes and Müller cells to increase retinal expression of IL-6-type cytokines such as CNTF, LIF, and IL-6.[5,14–16] Depletion of these cytokines using the respective genetic knockout compromises or even completely abolishes the regeneration-promoting effects of IS, thereby verifying their essential contribution to this approach.[5,16] Similarly, application of exogenous CNTF is neuroprotective and stimulates axon regeneration in the injured optic nerve, particularly upon continuous release from virally transduced cells.[16–20] However, cytokine-induced signaling is normally attenuated via intracellular negative feedback loops. For instance, PTEN inhibits PI3K activity, while SOCS3 compromises JAK/STAT3 pathway activation.[6,21,22] Consequently, removal of these intrinsic brakes, e.g. by PTEN knockout, is sufficient to promote remarkable axon regeneration.[6] Ancillary activation of gp130 signaling upstream of PTEN with either CNTF bolus injections or IS further increases the number and length of regenerating axons of PTEN-depleted RGCs.[23–25] However, this approach is unfavorable as therapeutic treatment, since it requires neuronal transduction weeks prior to CNS injury and might increase the risk of cancer development post-treatment.[17–19]

Instead of genetically deleting intracellular inhibitors, we hypothesized that it might be possible to boost axon regeneration by directly enhancing the cytokine-induced stimulus. In order to elicit a cellular response, CNTF and IL-6 first need to bind to their respective high affinity, but nonsignaling α-receptors (CNTFRα, IL-6Rα), which then recruit further signaling receptor subunits. In case of IL-6/IL-6Rα, these consist of a gp130 homodimer, while CNTF/CNTFRα signals via the gp130/LIFR heterodimer.[26] The response to CNTF or IL-6 is generally limited by low expression of the respective α-receptor subunits rather than gp130 expression.[26] In addition, CNTFRα

Correspondence: Dietmar Fischer, Division of Experimental Neurology, Medical Faculty, Heinrich-Heine-University Düsseldorf, Merowingerplatz 1a, 40225 Düsseldorf, Germany. E-mail: dietmar.fischer@uni-duesseldorf.de

is reportedly downregulated in RGCs upon axotomy, which would further decrease the responsiveness of these cells towards CNTF.[27] Alternatively, CNTF could signal via low-affinity binding to IL-6Rα on mature rat RGCs, which would however require much higher CNTF concentrations.[28] For these reasons, direct activation of gp130, which in the adult retina is mainly expressed in RGCs,[29] might be more efficacious than naïve cytokine application in eliciting robust neuroprotection and axon regeneration. Indeed, the current study demonstrates that direct stimulation of gp130 with hyper-IL-6 (hIL-6), a designer cytokine consisting of the covalently linked bioactive parts of IL-6 and soluble IL-6Rα,[30,31] potently induces activation of regeneration-relevant signaling pathways. Accordingly, hIL-6 supported longer neurite growth than CNTF or IL-6 in culture. More importantly, AAV-mediated retinal hIL-6 expression after optic nerve injury *in vivo* promoted stronger optic nerve regeneration than observed after either IS or RGC-specific PTEN knockout. To our knowledge, gp130 activation with hIL-6 is hence a single treatment with one of the so far strongest regeneration-promoting effects, which can be applied after axon injury. Thus, direct stimulation of gp130 with hIL-6 might be a clinically applicable approach to markedly improve regeneration after CNS injury.

RESULTS

Induction of gp130 signaling upon hIL-6 stimulation in CNS neurons

In non-neuronal cells, direct activation of gp130 with the designer cytokine hIL-6 induces stronger and longer-lasting intracellular signaling than naive IL-6-type cytokines.[31] We therefore intended to test whether hIL-6 might also induce stronger signaling in primary adult neurons and lead to increased axon regeneration. As continuous, longer-term release of natural cytokines has previously been shown to promote axon regeneration more effectively than intravitreal injections of high doses,[16–18] we opted for direct RGC-specific AAV transduction. This way, hIL-6 would be continuously released and could rapidly stimulate neurons via auto- and/or paracrine signaling *in vivo*. To this end, we cloned hIL-6 cDNA into an AAV2-GFP expression vector and initially evaluated hIL-6 expression and secretion in HEK293 cells. Expression of hIL-6 was detected post transfection by immunocytochemistry and Western Blot analysis using an antibody recognizing the IL-6-domain (**Figure 1a**,**b**). In addition, hIL-6 was efficiently secreted into the cell culture supernatant, which did not contain detectable levels of cytoplasmic proteins such as actin (**Figure 1b**). Conditioned medium was collected at 24 hours and used as a source of hIL-6 in subsequent experiments.

To test the biological activity of our hIL-6, we exposed dissociated mouse retinal cells including RGCs to increasing concentrations (10 pmol/l-1,000 nmol/l) and determined its effect on gp130-dependent signaling pathways (**Figure 1c**). In non-neuronal cells, hIL-6 can reportedly activate JAK/STAT, PI3K/AKT as well as MAPK/ERK signaling.[32] Consistently, STAT3 phosphorylation was already induced after 15 minutes incubation with 10 pmol/l hIL-6, but much stronger activation was achieved at concentrations ≥10 nmol/l. Similarly, increased AKT phosphorylation was detected ≥1 nmol/l (**Figure 1c**).

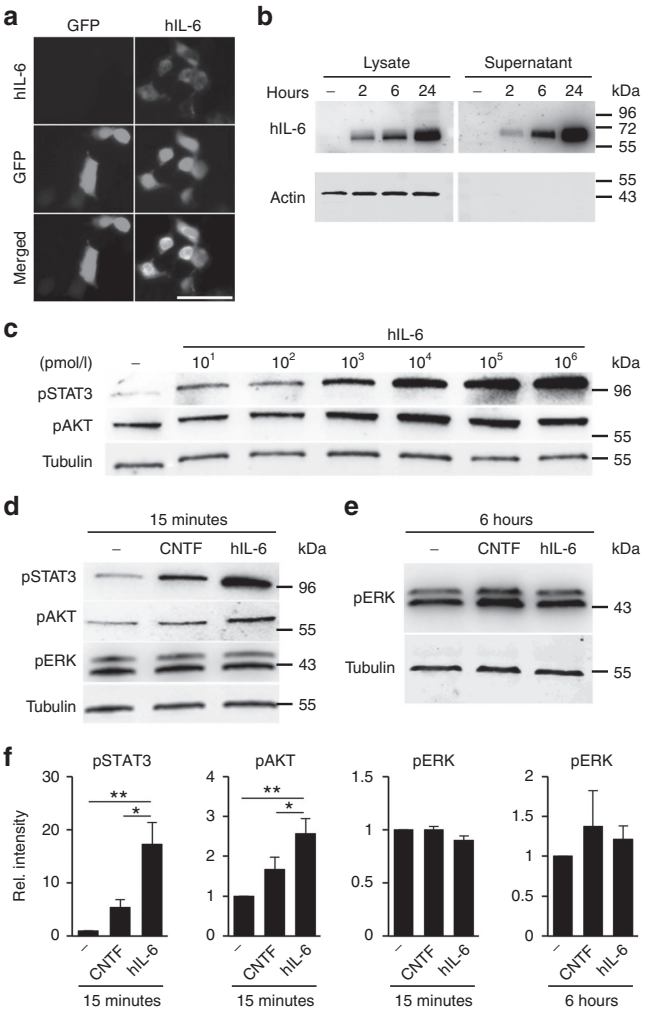

Figure 1 Generation of biologically active hIL-6. (**a**) HEK293 cells were transfected with either hIL-6 (right panel) or empty expression plasmid (green fluorecent protein; GFP, left panel) and stained with an antibody recognizing the IL-6 domain. Hyper-IL-6-positive cells were only detected upon hIL-6 transfection. Transfected cells were identified by GFP expression. Scale bar = 50 µm. (**b**) Hyper-IL-6 was specifically detected as a single band of ~60 kDa in lysates and supernatants of hIL-6 transfected HEK293 cells at 2, 6, and 24 hours after medium change, but not in untransfected cells (-) using an antibody recognizing the IL-6-domain. Recombinant hIL-6 was increasingly secreted into the supernatant. Actin served as loading control for cell lysates and its absence from supernatants ascertained hIL-6 secretion from intact cells. Numbers to the right indicate molecular weight markers. (**c**) Cultures of dissociated mouse retinal cells including retinal ganglion cells (RGCs) were either untreated (-) or exposed to various concentrations of hIL-6 (10 pmol/l–1 µmol/l) for 15 minutes. The respective cell lysates were subjected to Western blot analysis using antibodies against phosphorylated STAT3 (pSTAT3) and pAKT. Beta III-tubulin (Tubulin) served as loading control. (**d**,**e**) Western blots of retinal cultures either untreated (-) or incubated with 10 nmol/l CNTF or hIL-6 for 15 minutes (**d**) or 6 hours (**e**) and analyzed with antibodies against pSTAT3, pAKT, and pERK1/2, respectively. Beta III-tubulin served as loading control. (**f**) Densitometry of Western blots as shown in **d** and **e**. Incubation with 10 nmol/l hIL-6 stimulated stronger phosphorylation of pSTAT3 and AKT at 15 minutes compared to equimolar concentration of CNTF, whereas pERK1/2 levels were neither increased at 15 minutes nor at 6 hours. Treatment effects: $*P \leq 0.05$, $**P \leq 0.01$, n.s. = nonsignificant compared to untreated control.

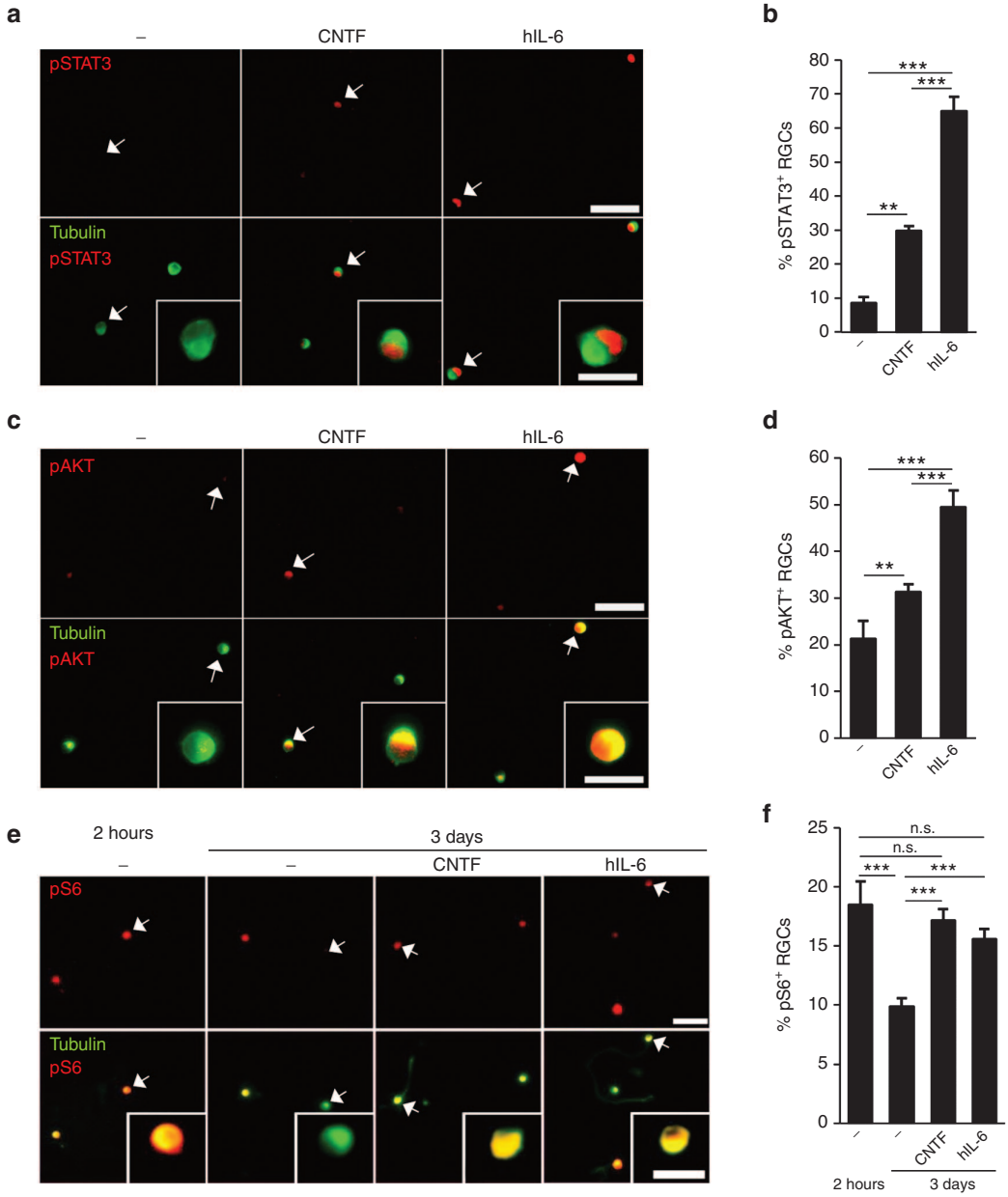

Figure 2 Activation of gp130-dependent signaling pathways in retinal ganglion cells (RGCs). (**a,c**) Representative pictures of mouse retinal cultures treated for 60 minutes with 10 nmol/l CNTF and hIL-6, respectively. RGCs were identified by βIII-tubulin antibody (green) and co-stained for either pSTAT3 (**a**) or pAKT (**c**). Both CNTF and hIL-6 induced phosphorylation of STAT3 and AKT in RGCs compared to untreated controls (-), but staining was significantly stronger (in numbers and intensity) in hIL-6-treated cultures. Scale bar = 50 µm, 15 µm for insets, showing selected cells (arrows) at higher magnification. (**b,d**) Quantification of RGCs positive for pSTAT3 (**b**) and pAKT (**d**), respectively, in retinal cultures as described in **a** and **c**. Treatment effects compared to untreated controls: $^{**}P \leq 0.01$, $^{***}P \leq 0.001$. (**e**) Dissociated RGCs either untreated (-) or incubated with 10 nmol/l CNTF or hIL-6 and stained for phosphorylated ribosomal protein S6 (pS6, red) and βIII-tubulin (green) at 2 hours and 3 days in culture. Scale bar = 50 µm, 15 µm for insets showing selected cells at higher magnification. (**f**) Quantification of retinal cultures as described in **e**. Treatment with either 10 nmol/l CNTF or hIL-6 prevented axotomy-induced downregulation of S6 phosphorylation. ***p<0.001; **p<0.01; n.s.= non-significant.

Induction of STAT3 and AKT phosphorylation by hIL-6 (10 nmol/l) was stronger compared to equimolar concentrations of CNTF (Figure 1d,f), suggesting higher efficacy of hIL-6. Quantification of pSTAT3- and pAKT-positive RGCs in retinal cultures confirmed stronger induction of the respective signaling pathways by hIL-6 compared to equimolar CNTF (Figure 2a–d). Interestingly, hIL-6 and CNTF both completely prevented the axotomy-induced decline of phosphorylated ribosomal protein S6, which serves as an indicator for mTOR activity[6,33] in cultured RGCs (Figure 2e,f). In contrast to STAT3- and AKT-phosphorylation, MAPK/ERK-signaling in dissociated RGCs remained unaffected by both CNTF and hIL-6 at 15 minutes and 6 hours after cytokine application (Figure 1d–f). Altogether, these data indicate that hIL-6 stimulates the JAK/STAT3- and PI3K/AKT-signaling pathways in mature RGCs more efficaciously than CNTF.

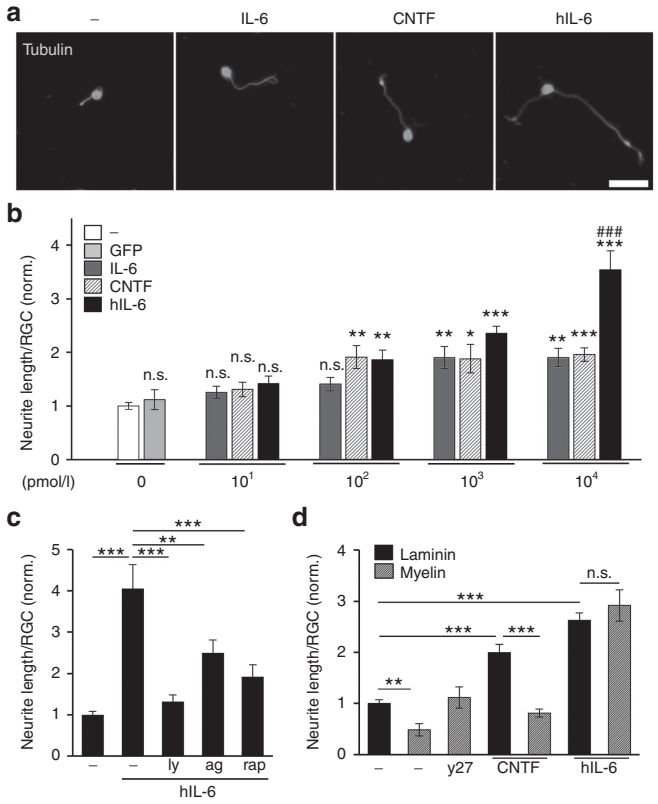

Figure 3 Efficient neurite growth of mature retinal ganglion cells (RGCs) upon hIL-6 stimulation. (**a**) Representative pictures of dissociated adult mouse RGCs cultured for 4 days either untreated (-) or in the presence of IL-6, CNTF or hIL-6 at 10^4 pmol/l and visualized by βIII-tubulin staining. Scale bar = 50 µm. (**b**) Quantification of RGC neurite length in retinal cultures treated with control-supernatant from empty plasmid-transfected HEK293 cells (GFP), various concentrations of hIL-6 supernatant, recombinant IL-6 or CNTF as depicted in **a**). Whereas control-supernatant showed no effect compared to untreated cultures (-), incubation with hIL-6 increased neurite growth concentration-dependently. In comparison to IL-6 and CNTF, hIL-6 was more efficacious ($^{###}P \leq 0.001$), as ~3.5 increased neurite growth was observed with 10 nmol/l hIL-6 compared to twofold increase with 10 nmol/l IL-6 and CNTF, respectively. Data were normalized to untreated controls (-) with an average axon length of 10.5 µm/neuron and represent means ± SEM of three independent experiments. Treatment effects compared to untreated controls: $^{*}P \leq 0.05$, $^{**}P \leq 0.01$, $^{***}P \leq 0.001$, n.s.=non-significant. (**c**) Quantification of neurite length of dissociated RGCs treated with 10 nmol/l hIL-6 either alone or in combination with 5 µmol/l PI3K inhibitor LY294002 (ly), 7 µmol/l JAK/STAT3 inhibitor AG490 (ag) or 10 nmol/l mTOR inhibitor rapamycin (rap). All signaling inhibitors significantly impaired neurite growth of hIL-6 treated RGCs, indicating that hIL-6 induced neurite growth depended on PI3K/AKT/mTOR and JAK/STAT3 signaling. Data were normalized to untreated controls with an average axon length of 8.6 µm/neuron and represent means ± SEM of three independent experiments. Treatment effects: $^{**}P \leq 0.01$, $^{***}P \leq 0.001$. (**d**) Quantification of neurite length of mouse RGCs cultured either on laminin or myelin in the presence of 10 nmol/l CNTF and hIL-6, respectively. The ROCK inhibitor Y27632 (y27) was used as positive control for disinhibition on myelin. Neurite growth on myelin was reduced compared to laminin in untreated control (-) and CNTF-treated cultures, but not after hIL-6 incubation, indicating a disinhibitory effect of hIL-6. Data were normalized to untreated controls on laminin with an average axon length of 9 µm/neuron and represent means ± SEM of three independent experiments. Treatment effects: $^{**}P \leq 0.01$, $^{***}P \leq 0.001$, n.s., = nonsignificant.

HIL-6 markedly promotes neurite growth of mature RGCs

We next investigated whether increased gp130-mediated signaling upon hIL-6 application might translate into enhanced neurite growth of adult RGCs. Compared to untreated controls, neurite length was significantly increased by hIL-6, while supernatant from cells transfected with empty vector had no effect (**Figure 3a**,**b**). Remarkably, 0.1 nmol/l hIL-6 or CNTF were sufficient to induce ~2-fold longer neurites compared to controls. In comparison, 1 nmol/l IL-6 was required to induce similar neurite growth, indicating the lower potency of the native cytokine. Whereas this doubling was the maximum growth level for CNTF and IL-6 even at higher concentrations, 10 nmol/l hIL-6 further increased neurite length up to >3.5-fold (**Figure 3a**,**b**). Thus, hIL-6 was more efficacious in activating gp130 signaling and stimulating neurite growth. To verify the dependence of hIL-6-stimulated neurite growth on gp130 signaling, we exposed RGC cultures to chemical inhibitors of the induced downstream signaling pathways JAK/STAT3 (AG490), PI3K/AKT (LY294002) and mTOR (rapamycin). Expectedly, all inhibitors significantly reduced hIL-6 stimulated neurite growth (**Figure 3c**), without affecting the survival of RGCs (data not shown).

We also cultured dissociated mouse RGCs on growth-inhibitory myelin to test whether hIL-6, similar to IL-6 might exert disinhibitory effects (**Figure 3d**). Neurite length of RGCs grown on myelin was reduced compared to laminin in untreated controls as well as in CNTF-treated cultures. In contrast, comparable outgrowth irrespective of the culture substrate was observed upon hIL-6 treatment (**Figure 3d**). Specificity of the myelin effect was verified by complete disinhibition in the presence of the ROCK inhibitor Y27632. Thus, compared to CNTF and IL-6, hIL-6 was more efficacious in promoting neurite growth and additionally able to overcome myelin inhibition.

HIL-6 potently promotes neurite growth of adult DRG neurons

Compared to adult RGCs, peripheral neurons have a higher intrinsic capacity for axon regeneration and a different cytokine receptor repertoire. To test their responsiveness towards hIL-6, we exposed dissociated DRG neurons to different concentrations of hIL-6 (**Figure 4**). We used only recombinant IL-6 as positive control in these experiments,[34] as CNTF did not significantly increase axon growth of murine DRG neurons. Both IL-6 and hIL-6 elicited a pronounced and concentration-dependent growth response. However, hIL-6 was again more potent than the naive cytokine, since maximum growth was observed at 0.1 nmol/l hIL-6, but 10 nmol/l IL-6 (**Figure 4a**,**b**). Similar to RGCs, gp130 signaling was transduced via JAK/STAT3 and PI3K/AKT/mTOR cascades, as LY294002, AG490 and rapamycin all significantly impaired hIL-6-induced axon growth (**Figure 4c**). Likewise, the inhibitory effect of myelin was abrogated by either hIL-6 or IL-6, similar to ROCK inhibition using the chemical inhibitor Y27632 (**Figure 4d**). The survival of DRG neurons was not affected by any of these treatments (data not shown). Thus, hIL-6-mediated gp130 signaling not only promoted neurite growth of mature RGCs with higher efficacy than CNTF and IL-6, but also stimulated growth

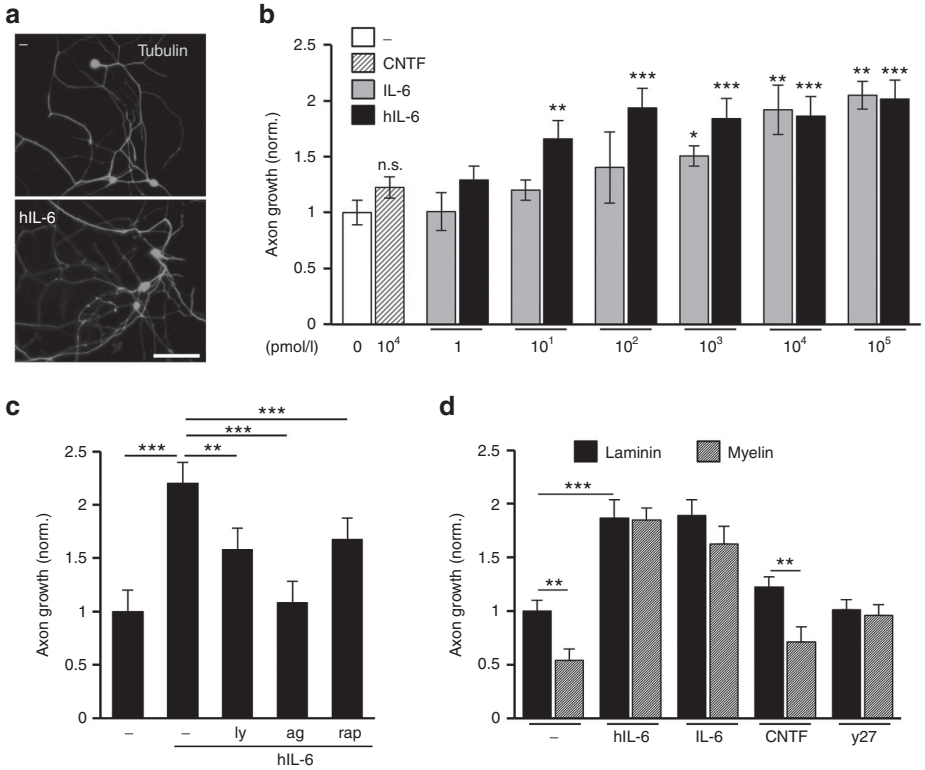

Figure 4 Axon growth stimulation in adult sensory neurons. (**a**) Representative pictures of dissociated adult mouse dorsal root ganglion (DRG) neurons cultured for 2 days either with vehicle control (-) or 10 nM hIL-6, visualized by βIII-tubulin staining. Scale bar = 100 µm. (**b**) Quantification of axon length in DRG cultures treated with 10 nmol/l CNTF and various concentrations of recombinant IL-6 or hIL-6 supernatant, respectively. Both IL-6 and hIL-6 induced axon growth concentration-dependently, with hIL-6 being significantly more potent than IL-6. CNTF had no effect compared to non-treated cells (-). Data were normalized to untreated controls with an average axon length of 1376 µm/neuron and represent means ± SEM of three independent experiments. Treatment effects: $*P<0.05$, $**P \leq 0.01$, $***P \leq 0.001$. (**c**) Quantification of axon length of dissociated DRG neurons treated with 10 nmol/l hIL-6 and either 5 µmol/l PI3K inhibitor LY294002 (ly), 5 µmol/l JAK/STAT3 inhibitor AG490 (ag) or 10 nmol/l mTOR inhibitor rapamycin (rap). All signaling inhibitors significantly impaired neurite growth in comparison to hIL-6-treated RGCs, indicating that hIL-6 activates PI3K/AKT/mTOR and JAK/STAT3 signaling. Data were normalized to untreated controls (-) with an average axon length of 374 µm/neuron and represent means ± SEM of three independent experiments. Treatment effects: $**P \leq 0.01$, $***P \leq 0.001$. (**d**) Quantification of neurite length of adult mouse DRG neurons cultured either on laminin or myelin in the presence of 10 nmol/l hIL-6, IL-6, CNTF and 40 µmol/l ROCK inhibitor Y27632 (y27), respectively. Neurite growth on myelin was reduced compared to laminin in untreated control (-) and CNTF-treated cultures, but not after treatment with either hIL-6, IL-6 or y27, indicating their disinhibitory effect. Data were normalized to untreated controls (-) with an average axon length of 1143 µm/neuron and represent means ± SEM of two independent experiments. Treatment effects: $**P \leq 0.01$, $***P \leq 0.001$.

of peripheral, regeneration-competent DRG neurons with higher potency than IL-6.

Strong and sustained activation of gp130 signaling *in vivo*

We next generated AAV2 particles for exogenous hIL-6 expression *in vivo* using the previously cloned expression plasmid (see **Figure 1**). Consistent with previous reports,[4,6] transduction rates of more than 90% were reproducibly achieved with this virus, based on AAV-driven coexpression of GFP in RGCs 3 weeks after virus injection (**Figure 5a**). Western blot analysis of retinal lysates revealed elevated phosphorylation of STAT3 upon AAV-hIL-6 transduction compared to AAV-GFP controls as early as 5 days after intravitreal injection (**Figure 5b**). This implies that gp130 signaling would be stimulated prior to the initiation of RGC death after an axotomy.[35] However, levels of pSTAT3 kept increasing at 14 and 21 days after intravitreal injection, indicating prolonged gp130 activation upon hIL-6 overexpression. On the other hand, increased phosphorylation of AKT and ERK1/2 was only detected at 14 and 21 days after AAV application (**Figure 5b**). In comparison to hIL-6 expression, RGC-specific PTEN knockout in AAV-Cre treated PTEN-floxed mice predominantly induced PI3K/AKT signaling and only negligible STAT3 phosphorylation (**Figure 5f**). Immunostaining of retinal cross sections confirmed upregulation of pSTAT3 in RGCs upon hIL-6 expression, while AAV-GFP had no effect (**Figure 5c**). This strong STAT3 activation upon AAV-hIL-6 transduction was observed despite expectedly increased expression of SOCS3, a known negative regulator of STAT3 (**Figure 5g**). Induction of AKT phosphorylation occurred specifically in RGCs, albeit later than for STAT3 (**Figure 5d**). In comparison, ERK1/2 activation was predominantly observed in glial cells rather than RGCs as indicated by co-staining with glial fibrillary acidic protein (GFAP) (**Figure 5e**). Overall, AAV transduction with biologically active hIL-6 promptly induced pronounced and sustained activation of gp130 signaling *in vivo* over at least several weeks.

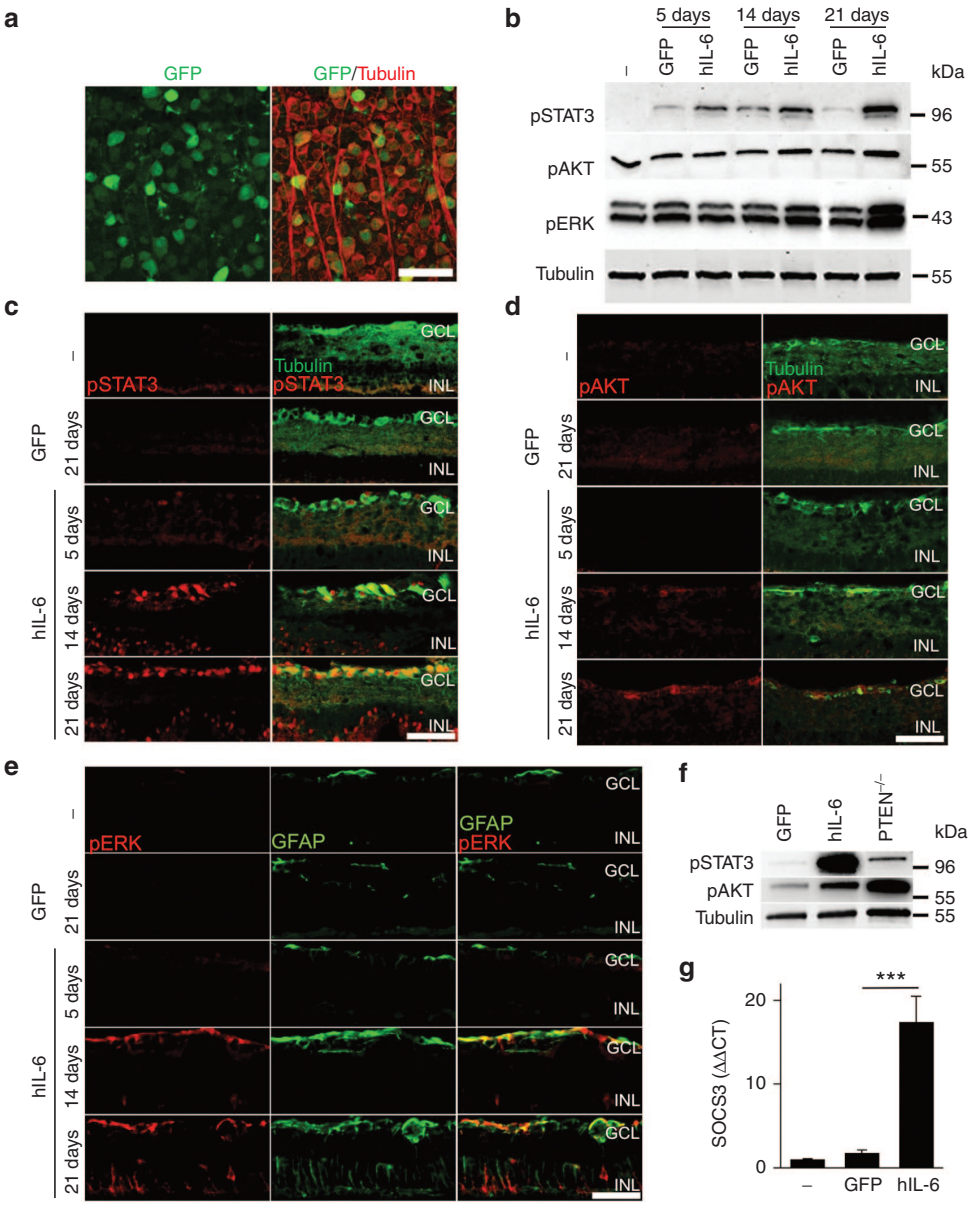

Figure 5 AAV-mediated expression of biologically active hIL-6 *in vivo*. (**a**) Retinal flat-mount 3 weeks after intravitreal application of AAV2-hIL-6. Expression of GFP (green) was detected in ~90% βIII-tubulin-positive retinal ganglion cells (RGCs) (red), indicating efficient transduction. Scale bar = 50 µm. (**b**) Western blots of retinal lysates from animals either untreated (-) or 5, 14, and 21 days post intravitreal injection of either AAV-hIL-6 (hIL-6) or AAV-GFP (GFP) with antibodies against phosphorylated STAT3 (pSTAT3), AKT (pAKT) and Erk1/2 (pERK). Beta III-tubulin served as loading control. Activation of STAT3, AKT and ERK upon hIL-6 expression occurred faster, stronger and longer compared to control-injected animals (GFP). (**c**) Immunohistochemical staining of cross-sections of untreated control retinae (-) and retinae isolated 5, 14, or 21 days after intravitreal injection of either AAV-GFP (GFP) or AAV-hIL-6 (hIL-6) with antibodies against pSTAT3 (red) and βIII-tubulin (green) to identify RGCs. AAV-mediated hIL-6 expression induced STAT3 phosphorylation in some RGCs already at 5 days after injection. At 21 days, almost all RGCs as well as some cells in the inner nuclear layer were pSTAT3-positive. Scale bar = 50 µm; GCL, ganglion cell layer; INL, inner nuclear layer. (**d**) Retinal cross-sections (as in **c**) stained with antibodies against pAKT (red) and βIII-tubulin (green). AAV-mediated hIL-6 expression markedly increased activation of AKT specifically in RGCs from 14 days after viral transduction. Scale bar = 50 µm; GCL, ganglion cell layer; INL, inner nuclear layer. (**e**) Retinal cross-sections (as in **c**) stained with antibodies against pERK1/2 (pERK, red) and glial fibrillary acidic protein (GFAP, green). pERK1/2 was predominantly induced in endfeet of Müller glia upon AAV-hIL-6 transduction. Moreover, GFAP expression was increased upon hIL-6 expression. Scale bar = 50 µm; GCL: ganglion cell layer; INL: inner nuclear layer. (**f**) Western blot analyses of retinal lysates from PTEN floxed mice 3 weeks after intravitreal injection of either AAV-GFP (GFP), AAV-hIL-6 (hIL-6) or AAV-Cre ($PTEN^{-/-}$) to induce PTEN knockout with antibodies against pSTAT3, pAKT and βIII-tubulin. Expression of hIL-6 predominantly induced STAT3 phosphorylation, while PTEN knockout strongly induced AKT phosphorylation in comparison to control injected animals. (**g**) Quantitative polymerase chain reaction analysis of SOCS3 expression in retinae 3 weeks after intravitreal injection of either AAV-GFP or AAV-hIL-6 in comparison to untreated controls (-). As expected, STAT3 activation upon hIL-6 expression markedly increased SOCS3 expression. Treatment effect: ***$P \leq 0.001$.

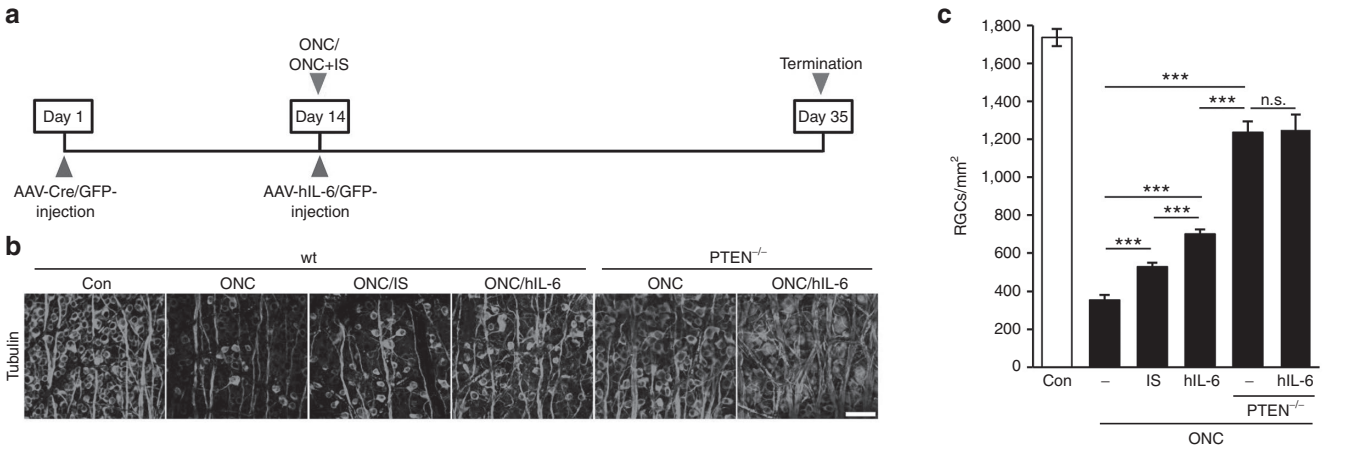

Figure 6 Neuroprotection upon hIL-6 expression. (**a**) Application scheme of the *in vivo* neuroprotection studies. Wild-type and PTEN floxed mice were intravitreally injected with either AAV-GFP or AAV-Cre. Two weeks afterwards, animals were subjected to optic nerve crush (ONC) and received intravitreal injections either with AAV-hIL-6 or AAV-GFP (-). Inflammatory stimulation (IS) and PTEN knockout (PTEN$^{-/-}$) served as positive controls. Numbers of surviving retinal ganglion cells (RGCs) were assessed 21 days after ONC. (**b**) Representative pictures of surviving, βIII-tubulin-positive RGCs in retinal flat-mounts treated as described in **a**. In contrast to hIL-6 treatment, knockout of PTEN significantly increased the size of surviving RGCs. A retina from untreated mice (con) is shown for comparison. Scale bar = 50 µm. (**c**) Quantification of surviving RGCs per mm^2 in retinal flat-mounts of mice treated as described in **a**). The neuroprotective effect of hIL-6 expression was significantly stronger than IS, but weaker than PTEN$^{-/-}$. Combination of hIL-6 and PTEN knockout had no additional neuroprotective effect. Treatment effects: ***$P < 0.001$, n.s., nonsignificant. Values represent means ± SEM of 5–8 retinae per treatment group.

AAV-hIL-6 application after nerve injury is neuroprotective and promotes extensive optic nerve regeneration

The impact of increased gp130 signaling on CNS regeneration was tested using the optic nerve crush (ONC) paradigm. Since hIL-6 was evidently more efficacious than CNTF in culture and promptly activated signaling cascades relevant for neuroprotection and axonal regeneration, we tested whether AAV-hIL-6 application directly after axonal lesion might be sufficient to elicit a positive response on neuronal survival and optic nerve regeneration *in vivo* (**Figures 6** and **7**). With respect to the development of a potential therapeutic treatment, this application scheme would be advantageous compared to previous studies deploying AAV-transductions for cytokine expression 1–3 weeks prior to injury.[17–19] At first, we analyzed potential neuroprotective effects of hIL-6 expression in comparison to AAV-GFP transduction as well as inflammatory stimulation (IS) and conditional PTEN knockout, two treatments reportedly protecting RGCs from injury-induced cell death.[7,9] Three weeks after ONC, only ~20% of βIII-tubulin-positive RGCs survived in control-injected retinae (353 ± 26 versus 1736 ± 45 RGCs/mm^2 in uninjured retinae), while 529 ± 21 RGCs/mm^2 were quantified in IS-treated retinae (**Figure 6b,c**). In comparison, hIL-6 expressing retinae contained 702 ± 24 surviving RGCs/mm^2, representing ~40% of original RGCs. Therefore, direct and sustained activation of gp130 upon delayed hIL-6 expression was significantly superior to IS in protecting RGCs upon ONC. However, RGC-specific PTEN depletion showed an even stronger neuroprotective effect with ~70% surviving RGCs (1,236 ± 57 RGCs/mm^2), which was not significantly enhanced by additional hIL-6 expression (1,249 ± 82 RGCs/mm^2) (**Figure 6b,c**).

Next, we compared the extent of optic nerve regeneration upon these treatments by quantifying CTB-labeled regenerated axons at various distances from the crush site on longitudinal optic nerve sections (**Figure 7**). Consistent with previous studies,[4,5] intravitreal injection of control AAV-GFP had no effect, as only very few axons were detected less than 1 mm distal to the lesion site 3 weeks after ONC (**Figure 7b-g**). Significant axon regeneration was observed upon IS, with a few axons extending beyond 2 mm past the lesion (**Figure 7b-g**), thereby confirming older reports.[4,33] In comparison, AAV-hIL-6 transduction dramatically increased the number as well as the length of regenerating axons, with some axons detectable at 3.5 mm (**Figure 7b–g**). Thus, hIL-6 expression upon AAV-hIL-6 injection was considerably more effective in promoting optic nerve regeneration than natural cytokines released upon IS. As the effect of direct gp130 activation upon AAV-hIL-6 transduction was so unexpectedly strong, we also compared the extent of axon regeneration with RGC-specific conditional PTEN knockout, which in combination with IS elicits one of the strongest regenerative responses reported so far.[24,25] Consistent with these previous reports, PTEN knockout via intravitreal AAV-Cre injection of floxed mice 2 weeks prior to ONC induced a strong regenerative response (**Figure 7b-g**). However, regeneration in the optic nerve remained significantly weaker compared to AAV-hIL-6 transduction after ONC, despite the stronger neuroprotective effect of the PTEN knockout (**Figure 6c**). We also tested whether combination of PTEN knockout with either IS or AAV-hIL-6 would further increase axon regeneration after ONC. To this end, PTEN-floxed mice received intravitreal injections of AAV-Cre and 2 weeks later, at the time of ONC, they received either IS (lens injury) or intravitreal injection with AAV-hIL-6. While axon regeneration of IS-treated PTEN knockout mice (**Figure 7b-g**) was comparable to AAV-hIL-6 treated wild-type mice, number and length of regenerating axons was further increased upon combination of AAV-hIL-6 and PTEN knockout (**Figure 7b-g**), with some axons reaching the

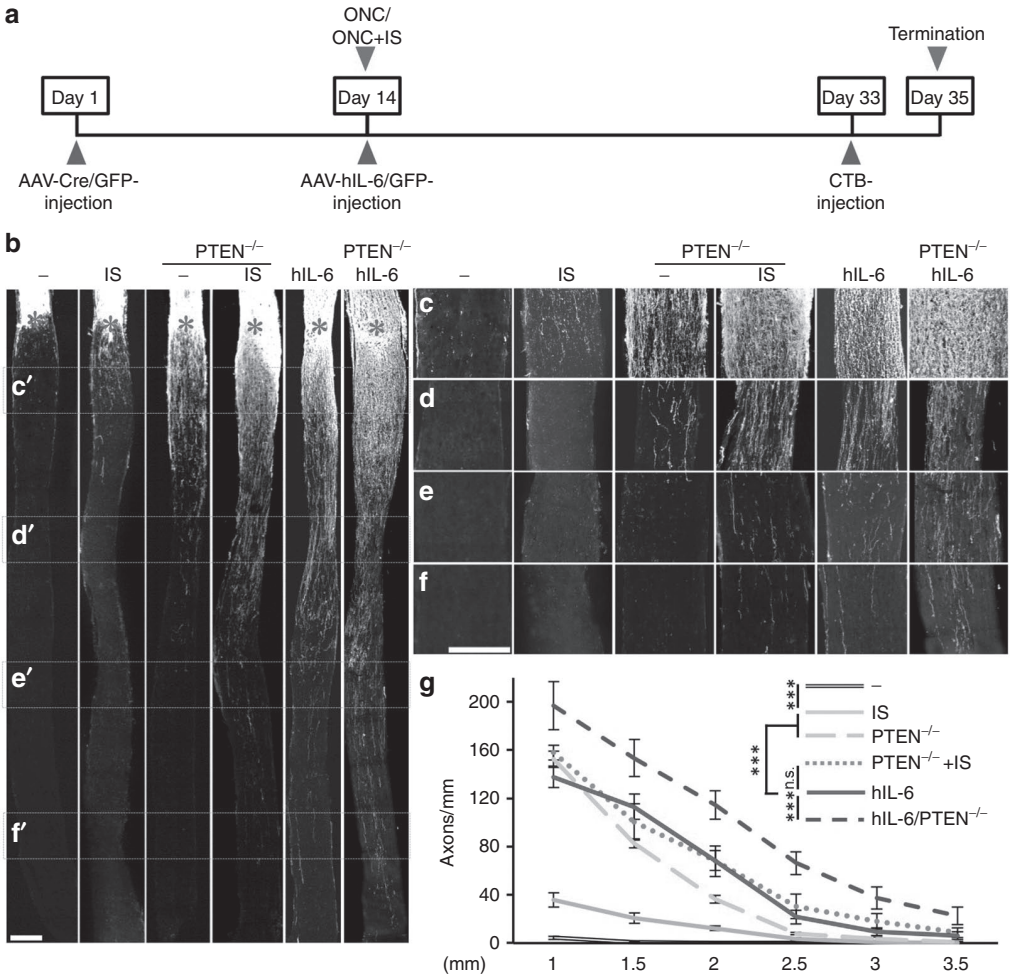

Figure 7 Markedly improved optic nerve regeneration upon hIL-6 expression. (**a**) Application scheme of the *in vivo* regeneration studies. Adult floxed PTEN mice were intravitreally injected either with AAV-Cre to induce RGC-specific PTEN deletion (PTEN$^{-/-}$) or with AAV-GFP (-) as control treatment 14 days prior to optic nerve crush (ONC). ONC was combined either with inflammatory stimulation (IS) or intravitreal injection of either AAV-hIL-6 or AAV-GFP. Fluorescently labeled cholera toxin (CTB) was injected 2 days prior to sacrifice at 3 weeks post ONC. (**b**) Representative pictures of longitudinal sections of optic nerves isolated from mice treated as depicted in **a**) with regenerating axons visualized by fluorescent CTB. Asterisks indicate the crush site. Scale bar = 200 µm. (**c–f**) Magnification of the respective optic nerve sections depicted in **b**), visualizing regenerating axons at 0.5 (**c**), 1.5 (**d**), 2.5 (**e**), and 3.5 mm (**f**) from the crush site. Scale bar = 200 µm. At 3.5 mm, axons are only detected in optic nerves of hIL-6, PTEN$^{-/-}$ + IS, and PTEN$^{-/-}$ + hIL-6. (**g**) Quantification of regenerating axons at 1, 1.5, 2, 2.5, 3, and 3.5 mm beyond the crush site in adult mice treated as described in **a**. Axon numbers were standardized to the width of the optic nerve at the respective distance from the lesion. Values represent means ± SEM of five to eight animals per treatment group. Treatment effects: ***$p \leq 0.001$, n.s. = nonsignificant.

optic chiasm already 3 weeks after ONC. This additive effect was restricted to axon regeneration, as it was not observed for RGC survival (**Figure 6c**). Overall, these data indicate that hIL-6 is so far one of the strongest single treatments for the promotion of optic nerve regeneration, which on its own is even as effective as PTEN knockout in combination with IS.

Sustained neuroprotection and axon regeneration upon prolonged hIL-6 expression

To investigate whether sustained hIL-6 expression would continue to stimulate optic nerve regeneration, we also quantified regenerating axons and surviving RGCs 6 weeks after ONC (**Figure 8**). Longitudinal optic nerve sections revealed a further increase in regenerating axons compared to 3 weeks after surgery. In addition, more axons were detected at longer distance, with considerable numbers now reaching the optic chiasm 4.5 mm beyond the lesion site (**Figure 8a,b**). Some regenerating axons were also detected within the optic chiasm and the contralateral optic nerve, implying pathfinding errors at this point of the retino-tectal projection as previously described.[24] In addition, hIL-6-transduced retinae still contained 2.6-fold more RGCs than control-injected animals (439 ± 35 versus 167 ± 13), representing a 25% survival rate 6 weeks after injury (**Figure 8c,d**). Therefore, continuous hIL-6 expression sustained axon regeneration and neuroprotection at prolonged time points after ONC.

DISCUSSION

Inflammatory stimulation or direct application of naïve IL-6 type cytokines are known to promote some neuroprotection and axon regeneration upon optic nerve injury in rodents.[2,5,17–19,36,37] However, these effects appear rather moderate in comparison to genetic depletion of SOCS3 or PTEN, which

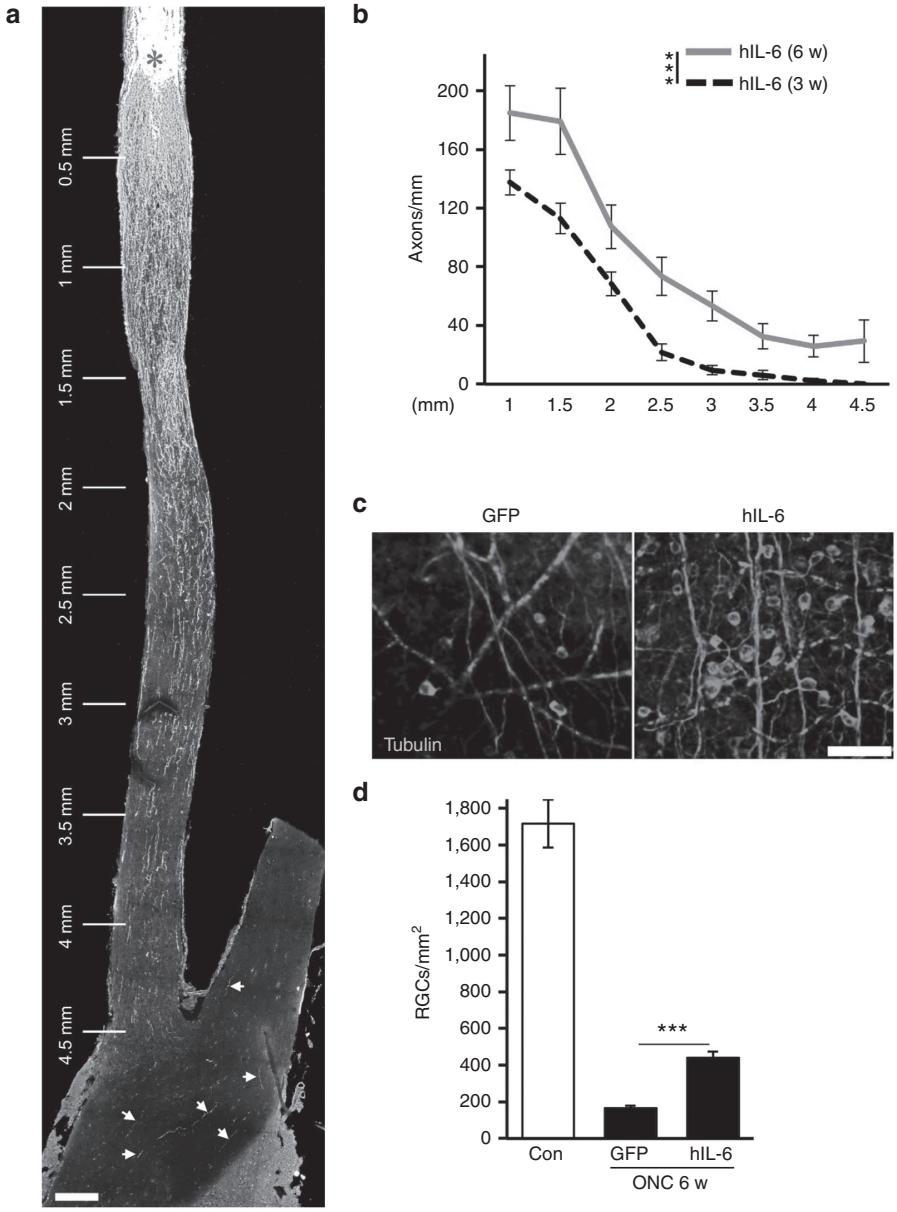

Figure 8 Regenerating axons enter the optic chiasm. (**a**) Representative longitudinal optic nerve section of an AAV-hIL-6-injected mice 6 weeks after optic nerve crush (ONC), with several regenerating axons in the optic chiasm and the contralateral optic nerve (arrows). The asterisk indicates the crush site. Scale bar = 200 µm. (**b**) Quantification of regenerating axons at 1, 1.5, 2, 2.5, 3, 3.5, 4, and 4.5 mm beyond the crush site in mice 6 weeks (w) after ONC and AAV-hIL-6 treatment. Axon numbers were standardized to the width of the optic nerve at the respective distance from the lesion and compared to regeneration at 3 weeks (dashed line, data from Figure 7) as reference. Treatment effects: ***$P \leq 0.001$. (**c**) Representative pictures of retinal flat-mounts from mice intravitreally injected with either AAV-GFP (GFP) or AAV-hIL-6 (hIL-6) showing surviving, βIII-tubulin-positive RGCs 6 weeks after ONC. Scale bar = 50 µm. (**d**) Quantification of surviving RGCs per mm^2 in retinal flat-mounts of mice treated as described in **c**). Retinae expressing hIL-6 still contain ~2.6 times more RGCs compared to AAV-GFP-injected control retinae. Data from untreated retinae (Con) are shown for comparison. Treatment effects: ***$P < 0.001$. Values represent means ± SEM of at least six retinae per treatment.

act as cell-intrinsic inhibitors of cytokine-induced signaling pathways.[6,21–23] Consequently, naive IL-6-type cytokines, released after IS or applied at high and sustained levels, are seemingly insufficient to induce optimal gp130 signaling in injured neurons. We therefore tested whether direct stimulation of endogenous gp130 receptors using the designer cytokine hIL-6 might be a superior, therapeutically applicable approach to induce robust signal pathway activation and CNS axon regeneration. Consistent with our hypothesis, hIL-6 activated gp130 dependent signaling pathways more efficaciously and elicited stronger axonal growth of cultured mature RGCs compared to CNTF and IL-6. Strikingly, sustained delivery of hIL-6 upon intravitreal AAV application right after optic nerve crush induced a stronger regenerative response *in vivo* than other previously described single treatments, with axons growing through the optic chiasm at 6 weeks after optic nerve crush. Thus, direct activation of gp130 signaling by hIL-6 is a novel approach with potential clinical relevance to robustly promote nerve regeneration.

Hyper-IL-6 reportedly activates various signaling cascades, including the JAK/STAT3, PI3K/AKT and MAPK/ERK pathways, in non-neuronal cells via direct binding to gp130.[36–38] Consistent with these previous results, hIL-6 promptly induced phosphorylation of STAT3 and AKT in cultured RGCs. Signal intensity as well as the number of positive RGCs were significantly higher compared to stimulation with CNTF. However, even stronger AKT phosphorylation was detected after RGC-specific PTEN knockout, indicating that direct gp130 stimulation via hIL-6, although more efficacious than CNTF, does not achieve maximum PI3K/AKT activation in neurons. On the other hand, PTEN knockout only slightly induced STAT3 phosphorylation compared to hIL-6 treatment. As both signaling pathways have been implicated in axon growth promotion,[23] it is conceivable that combination of hIL-6 with PTEN knockout led to even stronger optic nerve regeneration than either treatment alone. In contrast to JAK/STAT3 and PI3K/AKT signaling, hIL-6 did not measurably affect ERK1/2 phosphorylation in RGCs. Retinal ERK1/2 phosphorylation was restricted to astrocytes and the endfeet of Müller cells *in vivo* and earliest detected 2 weeks after viral injection. A similar activation pattern of the MAPK/ERK pathway was previously reported upon intravitreal injection of high doses of recombinant CNTF,[39] suggesting cell-specific gp130 activation profiles within the retina.[26,40] As MAPK/ERK pathway activation by AAV-mediated B-RAF overexpression reportedly promotes axon growth and enhances the effect of PTEN knockout on optic nerve regeneration,[41] a combinatorial treatment with hIL-6 and B-RAF might also lead to increased neuroprotection and regeneration. The outcome of such additional combinatorial approaches awaits further analyses.

Application of hIL-6 induced neurite growth of adult RGCs as well as DRG neurons similar to postnatal, gastrointestinal neurons in culture.[42] The observations that the JAK/STAT3 and PI3K/AKT/mTOR pathways were rapidly activated in low-density RGC cultures and that neurite growth promotion was compromised by the respective signaling pathway inhibitors strongly suggests a direct interaction of hIL-6 with gp130 on RGCs. In our assay, hIL-6 significantly enhanced neurite growth of RGCs from 0.1 nmol/l, which was equivalent to the potency of CNTF, but more potent than IL-6, which is consistent with previous reports.[31,43] However, only hIL-6 continued to increase neurite growth at concentrations ≥1 nM, indicating its higher efficacy compared to naive cytokines. This observation is consistent with high-affinity binding of CNTF to CNTFRα and IL-6 to IL-6Rα, respectively, but limited expression of CNTFRα, IL-6Rα and/or LIFR at the cell surface preventing maximal signal activation (**Figure 9**).[26,27] In comparison, higher concentrations of hIL-6 can enhance the growth stimulus further due to the wealth of gp130 receptors (**Figure 9**). Mouse DRG neurons only slightly responded to CNTF, but hIL-6 was again more potent than IL-6 in inducing neurite growth, which is consistent with previous reports for non-neuronal cells. In those studies, the increased potency of hIL-6 was attributed to its higher receptor binding affinity and the impaired internalization of activated signaling complexes.[31,43] The finding that hIL-6 was not more efficacious than IL-6 in DRG neurons could be due to the generally higher regenerative capacity of these PNS neurons that might require only moderate gp130 stimulation to maximally stimulate neurite growth. Detailed analysis of this aspect awaits further investigation.

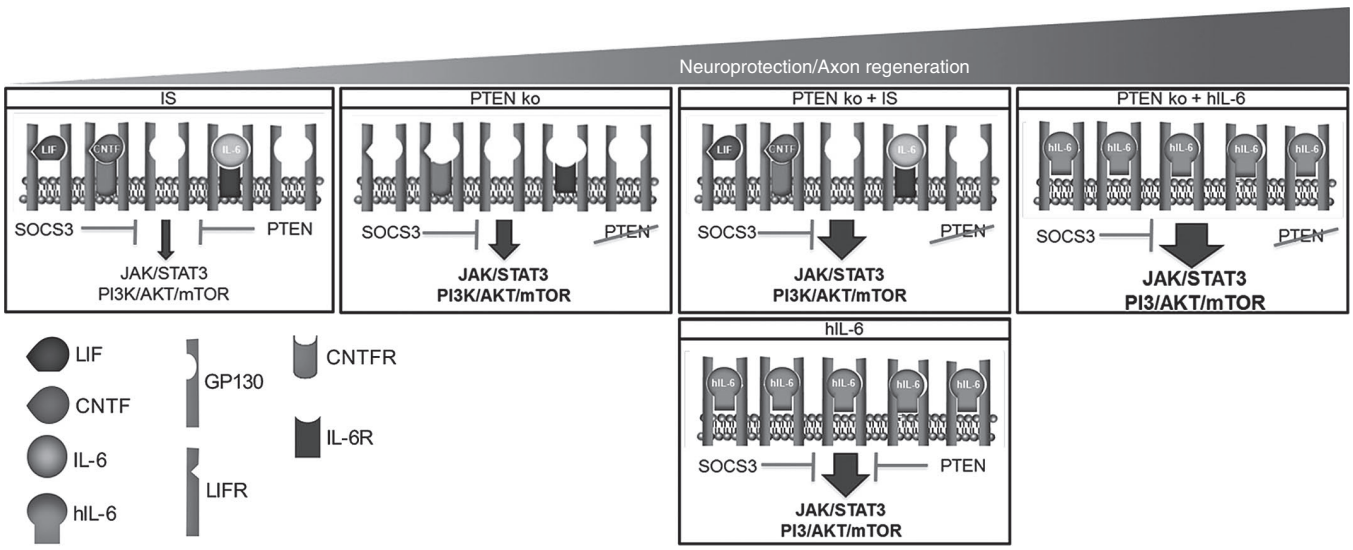

Figure 9 Schematic cartoon of gp130 signaling in various experimental settings. Inflammatory stimulation (IS) induces the release of different IL-6-like cytokines such as CNTF, LIF, and IL-6. These cytokines need to bind to their respective non-signaling α-receptors in order to activate ubiquitously expressed gp130. Activation of JAK/STAT3 and PI3K/AKT/mTOR signaling is restricted by the limited expression of α-and β-receptor subunits (leaving unbound gp130) and by the intrinsic inhibitors PTEN and SOCS3. Removal of the intrinsic brake on PI3K activity via PTEN knockout (PTEN ko, second panel) predominantly increases pAKT levels and promotes considerable axon regeneration. PTEN knockout in combination with increased release of native IL-6-like cytokines upon IS (PTEN ko + IS, third panel) stimulates gp130 signaling and accordingly increases the regenerative response after optic nerve injury in comparison to single PTEN knockout. Application of hIL-6 is expected to activate most gp130 receptors in neurons (lower panel), thereby causing a stronger stimulus. Despite ongoing presence of the intrinsic brakes PTEN and SOCS3, this strong activation of gp130-dependent signaling leads to optic nerve regeneration comparable to PTEN deletion combined with IS. However, additional PTEN depletion can further enhance axon regeneration (right panel).

Intravitreal application of AAV-hIL-6 after optic nerve crush markedly increased the number of surviving RGCs as well as optic nerve regeneration *in vivo*. As hIL-6 was efficiently secreted from HEK cells in culture, the induction of signaling cascades upon hIL-6 expression *in vivo* likely occurred via autocrine and paracrine activation of gp130 receptors. In support of this notion, pSTAT3 staining was detected only in few GFP-positive RGCs 5 days after intravitreal AAV application. At later time points, however, STAT3 activation was detected in almost all, even non-transduced RGCs as well as in some other retinal cells, most likely Müller cells and astrocytes. Concomitantly increased GFAP expression in these latter cells indicates their generally activated state, which might have indirectly contributed to the promotion of optic nerve regeneration *in vivo* at later stages. On the other hand, neurite growth stimulation and myelin disinhibition observed in cell culture rather support a direct effect of hIL-6 on RGCs.

Concerning the neuroprotective effect of hIL-6, about twice as many RGCs were still present in AAV-hIL-6-transduced compared to AAV-GFP-treated retinae 3 weeks after optic nerve injury and this effect was even more pronounced (2.6-fold) after 6 weeks. Thus, hIL-6-mediated neuroprotection was superior to IS, but inferior to RGC-specific PTEN knockout.[6] However, we did not address the possibility that AAV-hIL-6 application prior to optic nerve lesion, which would ensure higher hIL-6 expression levels upon injury, might lead to even stronger neuroprotection, as such an application scheme would be irrelevant for potential therapeutic treatments.

Regarding axon regeneration in the optic nerve, AAV-hIL-6 treatment after injury was significantly superior to IS or prophylactic RGC-specific PTEN knockout, thereby classifying direct gp130 activation as one of the so far best single treatments to promote axon regeneration. The observed effect was stronger than anticipated from the rather moderate increase of axonal growth *in vitro*, which could be attributed to the sustained expression and/or the additional disinhibitory effect of hIL-6 *in vivo*. Although AAV-hIL-6 was applied right after optic nerve lesion instead of prior to injury as described for previous experimental manipulations, the regenerative response was even comparable to levels achieved upon PTEN deletion in combination with CNTF application/IS.[6,23,41,44,45] Conceivably, it might be possible to further increase the number and length of regenerating axons by applying AAV-hIL-6 prior to injury or by using combinations with other previously reported genetic approaches,[23,35,41,46–50] as demonstrated by the combination of hIL-6 expression with RGC-specific PTEN knockout.

We chose to apply hIL-6 *in vivo* via AAV2 transduction of RGCs, since previous studies indicated that continuously released IL-6-type cytokines are more efficient in stimulating axon regeneration in the optic nerve than intravitreal injections of high doses of recombinant proteins.[5,16–20] In the future, this approach could be combined with an inducible system (*e.g.*, Tet on/off) to enable transient hIL-6 expression only during the regenerative phase.[51] Alternatively, hIL-6 delivery by encapsulated and therefore removable cells[52] might represent a promising therapeutic concept to promote axon regeneration upon nerve injuries in human patients. In addition to its potential therapeutic use, hIL-6 application also offers advantages for future regenerative research. For one, viral transduction after nerve injury significantly shortens the length of experimental studies. Moreover, the lens and vitreous body remain translucent upon AAV-hIL-6 transduction as opposed to zymosan injection or lens injury,[9,53] which is a prerequisite for future behavioral studies testing recovery of vision. Last, but not least, as hIL-6 also provoked strong growth promotion in regeneration-competent DRG neurons, this approach might be transferable to various other PNS and CNS injury paradigms. In particular, we are currently investigating whether direct activation of gp130 signaling would also improve the regenerative outcome upon spinal cord injury.

In conclusion, this study demonstrates that direct activation of gp130 signaling with hIL-6 is so far one of the most effective single treatments for the promotion of optic nerve regeneration. Robust neurite growth was elicited from different neuronal cell types in culture and the strong neuroprotection and remarkable axon elongation observed *in vivo* was comparable to previously described combinatorial treatments. In the future, this novel approach could not only enable broadened experimental regeneration studies, but also hold exciting promise for the development of clinically applicable therapeutic treatments to markedly improve regeneration after CNS injuries in human patients.

MATERIALS AND METHODS

Generation of biologically active hIL-6. The hIL-6 sequence was polymerase chain reaction (PCR)-amplified from a pCDM8 vector (kindly provided by Prof. Rose-John, Kiel, Germany) using primers 5′-GCC TAC CGC GGG TCG ACG CAT GGA-3′ and 5′-TAT AAT GCG GCC TAC ATT TGC CGA-3′ and cloned into an AAV2 expression vector under the control of a CMV promoter in front of an IRES:eGFP sequence (AAV-hIL-6). HEK293 cells were transfected with either AAV-hIL-6 or empty vector (AAV-GFP) as control. Cells were transferred to Dulbecco's modified Eagle medium (DMEM) without serum one day after transfection. Conditioned supernatants were collected after further 24 hours incubation and supplemented with 0.1% bovine serum albumin to stabilize hIL-6 protein. Concentrations of hIL-6 in supernatants were determined by Western blot analysis in comparison to serial dilution of human recombinant IL-6 (Serotec) using a polyclonal IL-6 antibody (ab6672, Abcam) with calculations as previously described.[31] Dilutions of hIL-6-conditioned medium were used for all subsequent cell culture experiments, with respective volumes of supernatant from GFP-transfected cells as negative controls.

Retinal cell cultures. Low-density retinal cultures were prepared as previously described.[54] In brief, dissected retinae were digested in DMEM (Invitrogen) containing 16.4 U/ml papain (Worthington) and 0.3 µg/ml L-cysteine (Sigma) at 37 °C for 30 minutes. Triturated retinae were washed with 50 ml DMEM to remove cell fragments and secreted factors. After centrifugation (500 g, 7 minutes) retinal cell pellets were resuspended in DMEM (1.5 ml/retina) containing B27-supplement (1:50, Invitrogen) and 200 U/ml penicillin/streptomycin (Biochrom) and plated into four-well tissue culture plates (Nunc) (300 µl/well) coated beforehand with poly-D-Lysine (0.1 mg/ml, molecular weight < 300,000 Da, Sigma) and laminin (20 µg/ml, Sigma). For some experiments, culture plates were additionally coated with inhibitory CNS-myelin extract as described before.[46,55] Cultures were treated with either control (GFP) or hIL-6 supernatant or with purified CNTF (Biotrend) or IL-6 (Peprotech) at various concentrations, 7 µmol/l JAK inhibitor AG490 (Calbiochem), 5 µmol/l PI3-kinase inhibitor LY294002 (Sigma), 10 nmol/l mTOR inhibitor rapamycin (LC Laboratories), or 10 µmol/l ROCK inhibitor Y27632 (Sigma) as indicated. Retinal cells were cultured for 4 days for neurite length analysis or as indicated for immunocytochemistry prior to fixation with 4%

paraformaldehyde (PFA) (Sigma). For Western blot analysis, cells were collected 15 minutes or 6 hours after treatment.

For neurite outgrowth assays, dissociated retinal cultures were stained with βIII-tubulin antibody (1:2,000 TUJ-1; BioLegend), a phenotypic marker for RGCs, as previously described.[12,16,35,47,56] All RGCs with neurites at least twice the length of the soma diameter were photographed under a fluorescent microscope (200×, Observer.D1, Zeiss) and neurite length was determined using ImageJ software. In addition, the total number of βIII-tubulin-positive RGCs with an intact nucleus, as judged by DAPI staining, was quantified per well to assess potential neurotoxic effects. Survival of RGCs was unaffected by any of the treatments. The average neurite length per RGC was determined by dividing the sum of neurite length by the total number of RGCs per well. Values were then normalized to the control group as indicated. Data represent the mean axon length per RGC ± SEM of four replicate wells per experiment and at least three independent experiments. Significances of intergroup differences were evaluated using one- or two-way analysis of variance (ANOVA), followed by multiple post hoc tests (Holm-Sidak, Tukey).

DRG cultures. DRG neurons were isolated from adult C57/BL6 mice as previously described.[57] In brief, DRG were harvested, digested with 0.25% trypsin/EDTA and 0.3% collagenase type IA (Sigma) in DMEM and mechanically dissociated. Cells were resuspended in DMEM containing 10% fetal bovine serum (GE Healthcare) and 500 U/ml penicillin/streptomycin (BioChrom) and cultured on 96-well plates coated beforehand with poly-D-Lysine (0.1 mg/ml, molecular weight < 300,000 Da, Sigma) and 20 µg/ml laminin (Sigma). Some of the culture plates were additionally coated with CNS-myelin extract.[46,58] Cell cultures were treated with 10 nmol/l CNTF, hIL-6 supernatant or purified IL-6 (Peprotech) at various concentrations, 5 µmol/l JAK inhibitor AG490 (Calbiochem), 5 µmol/l PI3-kinase inhibitor LY294002 (Sigma), 10 nmol/l mTOR inhibitor rapamycin (LC-Laboratories), or 40 µmol/l ROCK inhibitor Y27632 (Sigma) for 48 hours. Survival of DRG neurons was unaffected by any of these treatments. Cells were fixed in 4% PFA and stained with antibodies against NeuN (1:2,000 ab177487; Abcam) and βIII-tubulin (1:2,000; Covance). Quantifications of DRG neuron numbers and total axon length were automatically performed with the pathway microscope system (Biosciences) and corresponding Attovision software in six replicate wells per experimental group. Data represent mean axon length per DRG neuron ± SEM from at least two separate experiments, normalized to controls as indicated. Significances of intergroup differences were evaluated using ANOVA, followed by Holm-Sidak *post hoc* test.

Western blot analysis. Dissected mice retinae were homogenized in 75 µl lysis buffer (20 mmol/l Tris/HCl pH 7.5, 10 mmol/l KCl, 250 mmol/l sucrose, 10 mmol/l NaF, 1 mmol/l DTT, 0.1 mmol/l Na_3VO_4, 1% TritonX-100, 0.1% SDS) with protease inhibitors (Calbiochem) and phosphatase inhibitors (Roche) using five sonification pulses at 40% power (Bandelin Sonoplus). Dissociated RGCs were left untreated or incubated with either 10 nmol/l CNTF or hIL-6 at various concentrations for 15 minutes or 6 hours at 37 °C and 5% CO_2, pelleted by centrifugation (5 minutes at 900 g) and homogenized in 60 µl lysis buffer by sonication. HEK293 cell cultures medium was changed 24h after transfection. Cells were collected 2, 6, and 24 hours thereafter and homogenized in 100 µl lysis buffer. Cell lysates were centrifuged at 8,000 g for 10 minutes to remove cellular debris. Approximately 10 µg protein was separated per lane on 10% Mini TGX gels (BioRad) and transferred to nitrocellulose membranes (0.2 µm, BioRad) using the Trans-Blot Turbo system (BioRad). Blots were blocked in 5% dried milk in either Tris- or phosphate-buffered saline with 0.5% Tween-20 (TBS-T, PBS-T) for at least 1 hour at room temperature and then incubated either with polyclonal antibodies against IL-6 (1:1,000, ab6672, Abcam), phosphorylated (Tyr705) STAT3 (1:1,000, Cell Signaling Technology), phosphorylated (Thr308) AKT (1:1,000, Cell Signaling Technology), phosphorylated ERK1/2 (1:1,000, Cell Signaling Technology), β-actin (1:5,000; Sigma), or βIII-tubulin (1:1,000; BioLegend) in 5% bovine serum albumin in TBS-T at 4 °C overnight. Bound primary antibodies were visualized with anti-rabbit (1:80,000), anti-goat (1:20,000) or anti-mouse (1:80,000; all Sigma) immunoglobulin G (IgG) secondary antibodies conjugated to horseradish peroxidase using enhanced chemiluminescence substrate (Biozyme) on a FluoChemE detection system (ProteinSimple). Western Blots were repeated at least twice to confirm results and were densitometrically quantified using ImageJ software. For comparative quantification, band intensities were normalized to βIII-tubulin used as loading control and to respective untreated control groups.

RNA isolation and quantitative real-time PCR. Total RNA was isolated from mouse retinae using the RNeasy kit (Qiagen) according to the manufacturer's protocol. Retina-derived RNA (40 ng) was reverse transcribed using the superscript II kit (Invitrogen). Quantification of SOCS3 and glycerinaldehyd-3-phosphat-dehydrogenase (GAPDH) expressions was performed using SYBR Green PCR Master Mix (Applied Biosystems) and QuantiTect primers (Mm_SOCS3_2_SG, Mm_Gapdh_3_SG; QuantiTect Primer Assay, Qiagen) on an Applied Biosystems 7500 real-time PCR system. Retina-derived cDNA was amplified during 50 cycles according to the manufacturer's protocol. All reactions were performed in duplicate, and at least two independent samples (from different eyes) were analyzed per experimental group. The specificity of the PCR product was verified with the dissociation curve analysis feature.

Retinal and optic nerve cross sections. Mice were anesthetized and perfused through the heart with cold PBS followed by 4% PFA in PBS. Isolated eyes with attached optic nerve segments were post-fixed in 4% PFA for 6 hours, transferred to 30% sucrose at 4 °C overnight and embedded in Tissue-Tek (Sakura). Longitudinal sections of the optic nerve or retina (14 µm) were cut on a cryostat (Leica), thaw-mounted onto Superfrost plus slides (ThermoFisher) and stored at −80 °C until further use. Retinal sections were thawed, washed in PBS for 15 minutes and permeabilized by 10 minutes incubation in 100% Methanol (Sigma). Sections were stained with antibodies against pSTAT3 (1:200), pAKT-Thr308 (1:500), pERK1/2 (1:500) (all Cell Signaling Technology), GFAP (1:50; Santa Cruz Biotechnology) and βIII-tubulin (1:2,000; BioLegend). Secondary antibodies included anti-mouse and anti-rabbit Alexa Fluor 488 or 594, respectively (1:1,000, Invitrogen). Sections were embedded in Moviol and analyzed using a fluorescent microscope (Observer.D1, Zeiss). Representative pictures of each experimental group were taken on LSM510 confocal microscope (Zeiss).

Immunocytochemistry. Transfected HEK293 cells and primary neuronal cell cultures were fixed with 4% PFA for 30 minutes at room temperature, permeabilized by 10 minutes incubation in 100% Methanol (Sigma) and blocked with 2% bovine serum albumin/5% donkey serum in PBS-T. Cells were stained with antibodies against pSTAT3 (1:200), pAKT-Thr308 (1:500), pS6 (1:500), (all Cell Signaling Technology) and βIII-tubulin (1:2,000; BioLegend). Secondary antibodies included anti-mouse and anti-rabbit Alexa Fluor-488 or -594, respectively (1:1,000, Invitrogen) and staining was analyzed using fluorescent microscopy (Observer.D1, Zeiss).

Preparation of AAV2. AAV plasmids carrying either cDNA for Cre-HA (AAV-Cre, kindly provided by Dr. Zhigang He), hIL-6 or GFP downstream of a CMV promoter were cotransfected with pAAV-RC (Stratagene) encoding the AAV genes rep and cap and the helper plasmid (Stratagene) encoding E24, E4, and VA into AAV-293 cells (Stratagene) for recombinant AAV2 generation. Purification of virus particles was performed as described previously.[4] Mainly, RGCs are transduced upon intravitreal injection of AAV2 as this virus serotype is highly neurotropic and RGCs are the first neurons to be encountered by the virus upon intravitreal injection.

Optic nerve crush (ONC), inflammatory stimulation (IS), and intravitreal injection. All surgical procedures were approved by the local authorities (LANUV Recklinghausen) and conducted in compliance with federal and state guidelines for animal experiments in Germany as previously described.[5,39] In brief, 2–3 months old, homozygous PTEN floxed mice on

C57BL/6j background (Jackson Laboratories) (20–25 g) or corresponding wild type mice were anesthetized by intraperitoneal injection of ketamine (120 mg/kg) and xylazine (16 mg/kg). The optic nerve was surgically exposed under an operating microscope and crushed 1 mm behind the eye for 10 seconds using jeweler's forceps. The integrity of the retinal vasculature was verified by funduscopic examination after each surgery.

Inflammatory stimulation (IS) was induced by lens injury using a retrolenticular approach, puncturing the lens capsule with the tip of a microcapillary tube as described previously.[9] Mice received 2 µl intravitreal injections of either AAV-Cre or AAV-GFP 2 weeks prior to ONC, while AAV-hIL-6 or AAV-GFP were intravitreally injected directly after optic nerve crush. Each experimental group consisted of six to eight mice. Two days before the end of the study, 2 µl fluorescently labeled (Alexa Flour-555) cholera toxin subunit B (CTB, 0.5% in PBS; Invitrogen) was intravitreally injected as an anterograde tracer to visualize regenerated axons.

Assessment of neuroprotection. Surviving RGCs were quantified in retinal flat-mounts stained with βIII-tubulin antibody (1:1,000 TUJ-1, BioLegend) as previously described.[33] Four nonoverlapping pictures were taken in each retinal quadrant, proceeding from the center to the periphery. The number of βIII-tubulin-positive RGCs was determined from each picture and divided by the area size. Values were averaged per retina and across all similarly treated animals to obtain a group mean ± SEM. At least five retinae were analyzed per experimental group. Significances of intergroup differences were evaluated using two-way ANOVA, followed by corrections for multiple post hoc tests (Holm-Sidak, Tukey).

Optic nerve regeneration. Axon regeneration was quantified as described previously.[4,6] In brief, numbers of CTB-labeled axons were counted every half millimeter from the injury site on at least five longitudinal optic nerve sections per animal and normalized to the cross-sectional width of the optic nerve at this distance. Each experimental group included data from at least five mice. Significances of intergroup differences were evaluated using two-way ANOVA, followed by the Holm-Sidak *post hoc* test using GraphPad Prism software.

ACKNOWLEDGMENTS

We are grateful to Prof. Rose-John for providing the cDNA for hyper-IL6. We thank Marcel Kohlhaas for technical support. This work was supported by the German Research Foundation (DFG).

REFERENCES

1. Silver, J and Miller, JH (2004). Regeneration beyond the glial scar. *Nat Rev Neurosci* **5**: 146–156.
2. Fischer, D and Leibinger, M (2012). Promoting optic nerve regeneration. *Prog Retin Eye Res* **31**: 688–701.
3. Lu, Y, Belin, S and He, Z (2014). Signaling regulations of neuronal regenerative ability. *Curr Opin Neurobiol* **27**: 135–142.
4. Leibinger, M, Andreadaki, A, Diekmann, H and Fischer, D (2013). Neuronal STAT3 activation is essential for CNTF- and inflammatory stimulation-induced CNS axon regeneration. *Cell Death Dis* **4**: e805.
5. Leibinger, M, Müller, A, Andreadaki, A, Hauk, TG, Kirsch, M and Fischer, D (2009). Neuroprotective and axon growth-promoting effects following inflammatory stimulation on mature retinal ganglion cells in mice depend on ciliary neurotrophic factor and leukemia inhibitory factor. *J Neurosci* **29**: 14334–14341.
6. Park, KK, Liu, K, Hu, Y, Smith, PD, Wang, C, Cai, B *et al.* (2008). Promoting axon regeneration in the adult CNS by modulation of the PTEN/mTOR pathway. *Science* **322**: 963–966.
7. Hauk, TG, Leibinger, M, Müller, A, Andreadaki, A, Knippschild, U and Fischer, D (2010). Stimulation of axon regeneration in the mature optic nerve by intravitreal application of the toll-like receptor 2 agonist Pam3Cys. *Invest Ophthalmol Vis Sci* **51**: 459–464.
8. Fischer, D, Hauk, TG, Müller, A and Thanos, S (2008). Crystallins of the beta/gamma-superfamily mimic the effects of lens injury and promote axon regeneration. *Mol Cell Neurosci* **37**: 471–479.
9. Fischer, D, Pavlidis, M and Thanos, S (2000). Cataractogenic lens injury prevents traumatic ganglion cell death and promotes axonal regeneration both *in vivo* and in culture. *Invest Ophthalmol Vis Sci* **41**: 3943–3954.
10. Leon, S, Yin, Y, Nguyen, J, Irwin, N and Benowitz, LI (2000). Lens injury stimulates axon regeneration in the mature rat optic nerve. *J Neurosci* **20**: 4615–4626.
11. Pernet, V and Di Polo, A (2006). Synergistic action of brain-derived neurotrophic factor and lens injury promotes retinal ganglion cell survival, but leads to optic nerve dystrophy in vivo. *Brain* **129**(Pt 4): 1014–1026.
12. Lorber, B, Berry, M and Logan, A (2005). Lens injury stimulates adult mouse retinal ganglion cell axon regeneration via both macrophage- and lens-derived factors. *Eur J Neurosci* **21**: 2029–2034.
13. Baldwin, KT, Carbajal, KS, Segal, BM and Giger, RJ (2015). Neuroinflammation triggered by β-glucan/dectin-1 signaling enables CNS axon regeneration. *Proc Natl Acad Sci U S A* **112**: 2581–2586.
14. Lorber, B, Guidi, A, Fawcett, JW and Martin, KR (2012). Activated retinal glia mediated axon regeneration in experimental glaucoma. *Neurobiol Dis* **45**: 243–252.
15. Lorber, B, Berry, M, Douglas, MR, Nakazawa, T and Logan, A (2009). Activated retinal glia promote neurite outgrowth of retinal ganglion cells via apolipoprotein E. *J Neurosci Res* **87**: 2645–2652.
16. Müller, A, Hauk, TG and Fischer, D (2007). Astrocyte-derived CNTF switches mature RGCs to a regenerative state following inflammatory stimulation. *Brain* **130**(Pt 12): 3308–3320.
17. Leaver, SG, Cui, Q, Plant, GW, Arulpragasam, A, Hisheh, S, Verhaagen, J *et al.* (2006). AAV-mediated expression of CNTF promotes long-term survival and regeneration of adult rat retinal ganglion cells. *Gene Ther* **13**: 1328–1341.
18. Leaver, SG, Cui, Q, Bernard, O and Harvey, AR (2006). Cooperative effects of bcl-2 and AAV-mediated expression of CNTF on retinal ganglion cell survival and axonal regeneration in adult transgenic mice. *Eur J Neurosci* **24**: 3323–3332.
19. Pernet, V, Joly, S, Dalkara, D, Jordi, N, Schwarz, O, Christ, F *et al.* (2013). Long-distance axonal regeneration induced by CNTF gene transfer is impaired by axonal misguidance in the injured adult optic nerve. *Neurobiol Dis* **51**: 202–213.
20. Lingor, P, Tönges, L, Pieper, N, Bermel, C, Barski, E, Planchamp, V *et al.* (2008). ROCK inhibition and CNTF interact on intrinsic signalling pathways and differentially regulate survival and regeneration in retinal ganglion cells. *Brain* **131**(Pt 1): 250–263.
21. Smith, PD, Sun, F, Park, KK, Cai, B, Wang, C, Kuwako, K *et al.* (2009). SOCS3 deletion promotes optic nerve regeneration in vivo. *Neuron* **64**: 617–623.
22. Park, KK, Hu, Y, Muhling, J, Pollett, MA, Dallimore, EJ, Turnley, AM *et al.* (2009). Cytokine-induced SOCS expression is inhibited by cAMP analogue: impact on regeneration in injured retina. *Mol Cell Neurosci* **41**: 313–324.
23. Sun, F, Park, KK, Belin, S, Wang, D, Lu, T, Chen, G *et al.* (2011). Sustained axon regeneration induced by co-deletion of PTEN and SOCS3. *Nature* **480**: 372–375.
24. Luo, X, Salgueiro, Y, Beckerman, SR, Lemmon, VP, Tsoulfas, P and Park, KK (2013). Three-dimensional evaluation of retinal ganglion cell axon regeneration and pathfinding in whole mouse tissue after injury. *Exp Neurol* **247**: 653–662.
25. Kurimoto, T, Yin, Y, Omura, K, Gilbert, HY, Kim, D, Cen, LP *et al.* (2010). Long-distance axon regeneration in the mature optic nerve: contributions of oncomodulin, cAMP, and pten gene deletion. *J Neurosci* **30**: 15654–15663.
26. Heinrich, PC, Behrmann, I, Haan, S, Hermanns, HM, Müller-Newen, G and Schaper, F (2003). Principles of interleukin (IL)-6-type cytokine signalling and its regulation. *Biochem J* **374**(Pt 1): 1–20.
27. Miotke, JA, MacLennan, AJ and Meyer, RL (2007). Immunohistochemical localization of CNTFRalpha in adult mouse retina and optic nerve following intraorbital nerve crush: evidence for the axonal loss of a trophic factor receptor after injury. *J Comp Neurol* **500**: 384–400.
28. Garbers, C, Hermanns, HM, Schaper, F, Müller-Newen, G, Grötzinger, J, Rose-John, S *et al.* (2012). Plasticity and cross-talk of interleukin 6-type cytokines. *Cytokine Growth Factor Rev* **23**: 85–97.
29. Echevarria, F, Walker, C, Abella, S, Won, M and Sappington, R (2013). Stressor-dependent alterations in glycoprotein 130: implications for glial cell reactivity, cytokine signaling and ganglion cell health in glaucoma. *J Clin Exp Ophthalmol* **4**:.
30. Fischer, M, Goldschmitt, J, Peschel, C, Brakenhoff, JP, Kallen, KJ, Wollmer, A, Grotzinger, J, Rose-John, S (1997). A bioreactive designer cytokine for human hematopoietic progenitor cell expansion. *Nat Biotechnol* **1**: 142–145.
31. Peters, M, Blinn, G, Solem, F, Fischer, M, Meyer zum Büschenfelde, KH and Rose-John, S (1998). *In vivo* and *in vitro* activities of the gp130-stimulating designer cytokine Hyper-IL-6. *J Immunol* **161**: 3575–3581.
32 Silver, JS and Hunter, CA (2010). gp130 at the nexus of inflammation, autoimmunity, and cancer. *J Leukoc Biol* 88: 1145–1146.
33. Leibinger, M, Andreadaki, A and Fischer, D (2012). Role of mTOR in neuroprotection and axon regeneration after inflammatory stimulation. *Neurobiol Dis* **46**: 314–324.
34. Cao, Z, Gao, Y, Bryson, JB, Hou, J, Chaudhry, N, Siddiq, M *et al.* (2006). The cytokine interleukin-6 is sufficient but not necessary to mimic the peripheral conditioning lesion effect on axonal growth. *J Neurosci* **26**: 5565–5573.
35. Fischer, D, Petkova, V, Thanos, S and Benowitz, LI (2004). Switching mature retinal ganglion cells to a robust growth state in vivo: gene expression and synergy with RhoA inactivation. *J Neurosci* **24**: 8726–8740.
36. Leibinger, M, Müller, A, Gobrecht, P, Diekmann, H, Andreadaki, A and Fischer, D (2013). Interleukin-6 contributes to CNS axon regeneration upon inflammatory stimulation. *Cell Death Dis* **4**: e609.
37. Fischer, D (2010). What are the principal mediators of optic nerve regeneration after inflammatory stimulation in the eye? *Proc Natl Acad Sci USA* **107**: E8; author reply E9.
38. Nechemia-Arbely, Y, Shriki, A, Denz, U, Drucker, C, Scheller, J, Raub, J *et al.* (2011). Early hepatocyte DNA synthetic response posthepatectomy is modulated by IL-6 trans-signaling and PI3K/AKT activation. *J Hepatol* **54**: 922–929.
39. Müller, A, Hauk, TG, Leibinger, M, Marienfeld, R, and Fischer, D (2009). Exogenous CNTF stimulates axon regeneration of retinal ganglion cells partially via endogenous CNTF. *Mol Cell Neurosci* doi:10.1016/j.mcn.2009.03.002.
40. Taga, T (1997). The signal transducer gp130 is shared by interleukin-6 family of haematopoietic and neurotrophic cytokines. *Ann Med* **29**: 63–72.
41. O'Donovan, KJ, Ma, K, Guo, H, Wang, C, Sun, F, Han, SB *et al.* (2014). B-RAF kinase drives developmental axon growth and promotes axon regeneration in the injured mature CNS. *J Exp Med* **211**: 801–814.
42. Schäfer, KH, Mestres, P, März, P and Rose-John, S (1999). The IL-6/sIL-6R fusion protein hyper-IL-6 promotes neurite outgrowth and neuron survival in cultured enteric neurons. *J Interferon Cytokine Res* **19**: 527–532.

43. Rakemann, T, Niehof, M, Kubicka, S, Fischer, M, Manns, MP, Rose-John, S *et al.* (1999). The designer cytokine hyper-interleukin-6 is a potent activator of STAT3-dependent gene transcription *in vivo* and *in vitro*. *J Biol Chem* **274**: 1257–1266.
44. Liu, K, Lu, Y, Lee, JK, Samara, R, Willenberg, R, Sears-Kraxberger, I *et al.* (2010). PTEN deletion enhances the regenerative ability of adult corticospinal neurons. *Nat Neurosci* **13**: 1075–1081.
45. Park, KK, Liu, K, Hu, Y, Kanter, JL and He, Z (2010). PTEN/mTOR and axon regeneration. *Exp Neurol* **223**: 45–50.
46. Sengottuvel, V, Leibinger, M, Pfreimer, M, Andreadaki, A and Fischer, D (2011). Taxol facilitates axon regeneration in the mature CNS. *J Neurosci* **31**: 2688–2699.
47. Fischer, D, He, Z and Benowitz, LI (2004). Counteracting the Nogo receptor enhances optic nerve regeneration if retinal ganglion cells are in an active growth state. *J Neurosci* **24**: 1646–1651.
48. Belin, S, Nawabi, H, Wang, C, Tang, S, Latremoliere, A, Warren, P *et al.* (2015). Injury-induced decline of intrinsic regenerative ability revealed by quantitative proteomics. *Neuron* **86**: 1000–1014.
49. Yungher, BJ, Luo, X, Salgueiro, Y, Blackmore, MG and Park, KK (2015). Viral vector-based improvement of optic nerve regeneration: characterization of individual axons' growth patterns and synaptogenesis in a visual target. *Gene Ther* **22**: 811–821.
50. Sengottuvel, V and Fischer, D (2011). Facilitating axon regeneration in the injured CNS by microtubules stabilization. *Commun Integr Biol* **4**: 391–393.
51. Bockamp, E, Maringer, M, Spangenberg, C, Fees, S, Fraser, S, Eshkind, L *et al.* (2002). Of mice and models: improved animal models for biomedical research. *Physiol Genomics* **11**: 115–132.
52. Tao, W, Wen, R, Goddard, MB, Sherman, SD, O'Rourke, PJ, Stabila, PF *et al.* (2002). Encapsulated cell-based delivery of CNTF reduces photoreceptor degeneration in animal models of retinitis pigmentosa. *Invest Ophthalmol Vis Sci* **43**: 3292–3298.
53. Yin, Y, Cui, Q, Li, Y, Irwin, N, Fischer, D, Harvey, AR *et al.* (2003). Macrophage-derived factors stimulate optic nerve regeneration. *J Neurosci* **23**: 2284–2293.
54. Grozdanov, V, Müller, A, Sengottuvel, V, Leibinger, M and Fischer, D (2010). A method for preparing primary retinal cell cultures for evaluating the neuroprotective and neuritogenic effect of factors on axotomized mature CNS neurons. *Curr Protoc Neurosci* **Chapter 3**: Unit3.22.
55. Ahmed, Z, Mazibrada, G, Seabright, RJ, Dent, RG, Berry, M and Logan, A (2006). TACE-induced cleavage of NgR and p75NTR in dorsal root ganglion cultures disinhibits outgrowth and promotes branching of neurites in the presence of inhibitory CNS myelin. *FASEB J* **20**: 1939–1941.
56. Fournier, AE and McKerracher, L (1997). Expression of specific tubulin isotypes increases during regeneration of injured CNS neurons, but not after the application of brain-derived neurotrophic factor (BDNF). *J Neurosci* **17**: 4623–4632.
57. Gobrecht, P, Leibinger, M, Andreadaki, A and Fischer, D (2014). Sustained GSK3 activity markedly facilitates nerve regeneration. *Nat Commun* **5**: 4561.
58. Heskamp, A, Leibinger, M, Andreadaki, A, Gobrecht, P, Diekmann, H and Fischer, D (2013). CXCL12/SDF-1 facilitates optic nerve regeneration. *Neurobiol Dis* **55**: 76–86.